


SUSTAINABLE SOLUTIONS AT TIMES OF TRANSITION ⋄ SUST. NISYROS, 15-17.09.2025

BOOK OF PAPERS

S5. Aegean Volcanic Arc

CONTENTS

PARAMETRIC STUDY OF THE THERMAL-HYDRAULIC CHARACTERISTICS OF DEEP BOREHOLE CO-AXIAL HEAT EXCHANGER IN A GEOTHERMAL WELL

Paige Draper[1,2], Ahmet T. Kalkisim[1], Ján Kubačka[1], Ken Seymour[2] and Tassos G. Karayiannis[1]

[1]Centre for Energy Efficient and Sustainable Technologies, Brunel University of London

[2] Pennmen Ltd, London W1J

email:tassos.karayiannis@brunel.ac.uk

ABSTRACT

Geothermal energy constitutes an additional option for energy planners and can have significant advantages when compared to other renewable sources. The work presented here relates to geothermal wells located in areas of average and high geothermal gradients, i.e. 30 and 80 K/km thermal diffusivity of 9.27 m^2/s and a soil temperature of 12 ^oC, as an average value. A closed-loop 3 and 5 km deep borehole co-axial heat exchanger was modelled using in-house developed software (WellTH). Water flows into the annulus space of the heat exchanger and upwards in the inner pipe. Studies were conducted for two different types of commercially available inner upward flow pipes, namely a High-Density Polyethylene (HDPE) and a vacuum-insulated tubing (VIT). The mass flow rate was varied from 1 to 15 kg/s. The water inlet temperature ranged from 10 to 80 ^oC to allow for the varying return temperature from possible different heating or power plants using the geothermal energy at ground level. Results are presented in the form of outlet temperature and thermal output as a function of the inner pipe insulation, mass flow rate, and water inlet temperature for operational periods up to 30 years and demonstrate the importance of these parameters. The pressure drop in the heat exchanger and the power required at the pump are included in the analysis. Finally, the possible output in terms of electricity production and heating using a heat pump are calculated.

Keywords: Geothermal energy, co-axial deep borehole, closed-loop, electricity generation, heating

1. INTRODUCTION

Energy demand for heating/cooling and electricity generation continues to rise due to population growth, the effort to increase quality of life and the proliferation of technologies such as electric vehicles, mobile devices and high-performance computing facilities [1]. In response, and bearing in mind the related environmental issues, governments and major technology companies are increasingly investing in renewable energy sources, including solar, wind and geothermal energy [2], [3]. Given the intermittency of solar and wind, supplying continuous electricity typically requires hybridisation with storage systems. Recently, policymakers recognized the importance of developing renewable energy sources that combine low carbon footprints with reliable, continuous operation. Among renewables, geothermal energy stands out due to its inherently low life-cycle carbon footprint and its ability to provide continuous electricity without the need for storage [4], [5]. This feature offers a strategic advantage for countries seeking to reduce reliance on imported petroleum products, a resource that frequently creates asymmetric dependencies and energy security risks. Unlike fossil fuels, which require geographic availability or international trade, renewable systems can be developed domestically, offering both energy independence and sustainability.

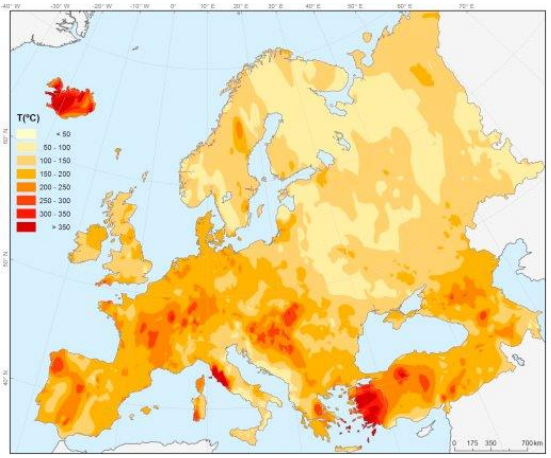

Figure 1: Formation temperatures across Europe at 5.5 km depth [9]

In Europe, geothermal energy is increasingly integrated into climate and energy policies. France has announced an ambitious action plan to expand both shallow and deep geothermal deployment. In 2021, renewable heat represented only ~1% (roughly 6 TWh) of nationwide heating demand, but the national target is to increase this share to 38% by 2030 [6], [7]. Similar policy initiatives and pilot projects are advancing in Germany, Netherlands, Italy, Finland, Turkiye and Belgium, while outside Europe, countries such as Indonesia, Iceland, Mexico and the United States are scaling geothermal capacity to diversify energy supply [5], [8]. Technological innovations are also accelerating adoption. Taken together, these developments underscore the growing importance of geothermal energy in the global transition toward sustainable, low-carbon, and secure energy systems. Figure 1 shows the diversity of the geothermal landscape in Europe, with significant variation in temperature gradients depending on location. At depths of 5.5 km, formation temperatures range from approximately 50 °C in regions with low gradients to over 350 °C in high-gradient areas, creating opportunities for both heating and electricity generation applications across the continent.

Geothermal energy derives from magmatic heat, radiogenic heat from radioactive decay, and conductive fluids, with temperature increasing with depth according to the local geothermal gradient [5], [10]. Exploiting this resource typically involves drilling deep wells and circulating working fluids through pipe systems to capture subsurface heat. Such configurations, demonstrated in Figure 2, are classified as deep-well systems. The open-loop systems include conventional hydrothermal systems exploiting the presence of naturally occurring aquifers or porous rocks. Enhanced Geothermal Systems involve stimulating the formation, which is not of desirable permeability, to create man-made fractures to allow for fluid flow between the wells. Closed-loop deep wells, i.e. (c) and (d) in Figure 2, isolate the working fluid from direct contact with the reservoir. Closed-loop systems mitigate risks of reservoir depletion, seismic activity, and groundwater contamination, offering a more environmentally secure solution. In cases where the energy available is used for heating purposes, they can be located near the required users (domestic as in district heating, agricultural or industrial parks). Recent studies highlight the potential of these closed-loop geothermal systems to deliver sustainable, low-carbon electricity [10], [11].

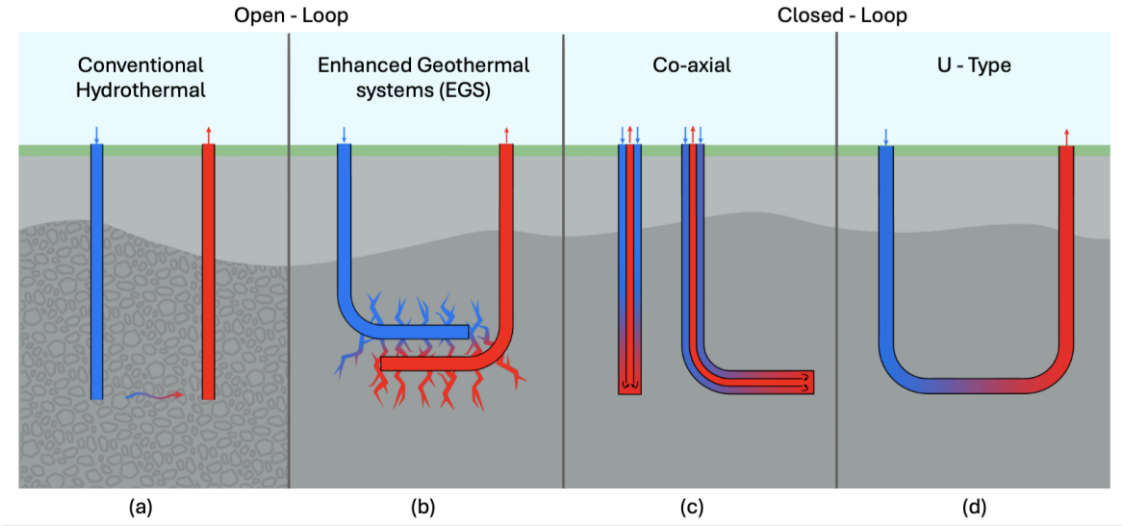

Figure 2: Types of geothermal installations (adapted from [12]).

Extensive research was conducted and published on deep well geothermal systems describing efforts to design feasible geothermal plants that extract heat from either hot rock layers or underground hot water in systems similar to Figure 2 and distribute it to district heating networks or power plants [13], [14]. Recently there is an increasing interest in repurposing abandoned oil and gas wells. It is estimated that there are 20 to 30 million world-wide [15]. Their use saves both time and drilling cost, with the latter estimated to be 75% of the total project cost of a geothermal plant [16]. Therefore, this business model seeks to convert existing boreholes into a heat source using efficient and practical methods [17], [18].

2. METHODOLOGY

2.1 Modelling and Validation

The objective of this study is to investigate the thermal hydraulic performance of co-axial DBHE systems, Figure 2(c) with no horizontal sections, that can be used in abandoned oil and gas wells and newly drilled ones, under different operating conditions and geological settings. A parametric analysis is conducted using an in-house software (WellTH) for well depths of 3 km and 5 km, considering variations in flow rate, inlet temperature, geothermal gradient, and internal pipe material. The study evaluates the long-term thermal output, outlet temperatures, pumping power requirements, and applicability for both direct heating and power generation over an operational period of up to 30 years.

The in-house *WellTH* software, see Kubačka and Karayiannis [10] and Kubačka [19], is a thermal-hydraulic simulation software written in C language dedicated to the assessment of the complex tasks related to the operation of coaxial and multilateral U-shaped deep bore heat exchangers (DBHEs), and well drilling and thru-tubing abandonment processes, [19]. The model incorporates both a numerical transient solution (TS) for heat transfer in the surrounding rock and its coupling with fluid flow in the annulus using a finite difference method. Additionally, the quasi-steady-state (QSS) approach as outlined in [10] and [19] was also employed. This method is based on the use of the radius of influence (ROI) concept to estimate heat transfer within the formation, allowing for significantly faster simulation times, while maintaining sufficient accuracy, which provides an advantage for large parametric sweeps where all parameters are time invariant.

The ROI method introduces time dependence into a steady-state model by defining a growing thermal influence region around the borehole, which increases thermal resistance and simulates the decreasing heat extraction rate due to thermal depletion. This approach is based on the line-source model, which assumes an infinite vertical heat source with radial heat conduction in a homogeneous medium. The QSS approach was also used by Alimonti [20] and Kujawa [21]. The ROI is calculated using Equation 1, see [19] for more details.

$$ROI = 2\sqrt{a\tau} \quad (1)$$

An extended description of the methodology used, i.e. resistance equation of all solid surfaces including the rock formation and the fluid flow convective heat transfer correlations used to calculate the heat transfer to/from the casing and inner tubing walls to the fluid is included is in [10]. Minor pressure losses within the DBHE are disregarded i.e. those occurring within the surface-to-the well infrastructure are disregarded as well as at the bottom turn, where flow transitions from the annulus to the tubing. An initial assessment was performed. The effect of axial nodalisation, i.e. calculation points per metre along the depth of the heat exchanger, was assessed. It was found that one node per metre resulted in adequate prediction accuracy in reasonable simulation time, see also [10]. The WellTH QSS method described above was validated using data from Bu et al. [22]. The authors produced a numerical model which was validated against data from an experimental 2,605 m co-axial DBHE in Qingdao China. In comparison the WellTH QSS method showed good agreement as seen in Figure 3 maintaining around 1% relative difference in outlet temperature with Bu et al.'s numerical model for all time steps. See [19] for further validation cases.

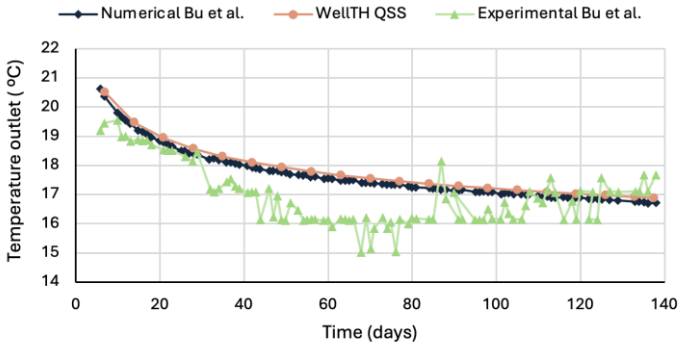

Figure 3: Comparison of WellTH QSS results with Bu et al's [22], 2,605m DBHE with 5°C, 30 m3/h inlet.

2.1. Well design and parameters

Figure 4 illustrates the geometry of the DBHE installation. The external casing was selected to represent a typical casing type and corresponding borehole diameter commonly used in hydrocarbon wells. It was assumed to remain uniform along the entire length of the DBHE. The thermal conductivities of the casing steel and cement were assumed to be 54 W/mK and 1.1 W/mK, respectively. The surrounding geological formation was modelled as a single homogeneous layer with a thermal conductivity of 2.4 W/mK, density 2590 kg/m^3 and specific heat capacity 1000 J/kg K giving a thermal diffusivity of 9.27×10^{-7} m²/s. Two types of central tubing were considered: (a) high-density polyethylene (HDPE) and (b) vacuum-insulated tubing (VIT). The dimensions and thermal conductivities for both configurations are sourced from [10], with specific diameters detailed in Table 1. The thermal conductivity of HDPE was taken as 0.54 W/mK, while the effective thermal conductivity of the VIT was assumed to be 0.0622 W/mK. This value was based on an internal air gap pressure of 10 Pa and an emissivity of 0.03 on both internal surfaces, corresponding to an aluminium coating. Further details regarding the design assumptions, the effects of pressure and emissivity in the VIT and the governing equations can be found in [10].

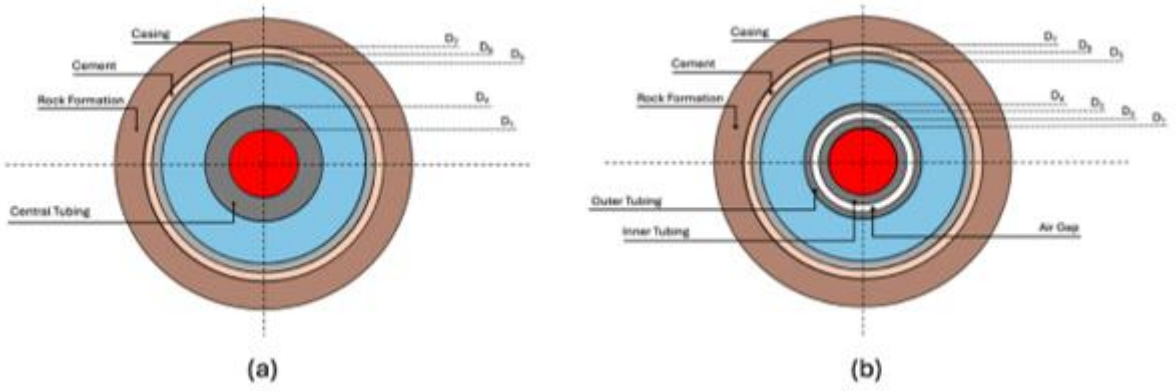

Figure 4: Co-axial DBHE cross- section for (a) HDPE internal tubing and (b) VIT internal tubing

Table 1: DBHE cross sectional diameters relating to Figure 4.

	D_1	D_2	D_3	D_4	D_5	D_6	D_7
Value (m)	0.0883	0.1016	0.11862	0.1397	0.2238	0.2445	0.3111

3. RESULTS AND DISCUSSION OF THE PARAMETRIC ANALYSIS

3.1. Effect of mass flow rate

The mass flow rate was varied between 1 kg/s and 15 kg/s for both well depths (3 km and 5 km). As depicted in Figure 5, both thermal output and outlet temperature decrease over time for all flow rates, with the steepest declines occurring in the early years of operation, reflecting rapid heat depletion in the surrounding formation. The decline in thermal output increases with flow rate, i.e. between year 1 and 30, thermal output drops by approximately 7% and 3% at 1 kg/s, and by 30% and 29% at 15 kg/s for the 3 km (a) and 5 km (c) DBHEs, respectively. Outlet temperature exhibits a similar trend, except with a percentage change peaking at intermediate flow rates. The maximum percentage decrease occurs at 6 kg/s (16%) and 11 kg/s (19%), after which the rate of decline slows and reaches 12.8% and 18.6% at 15 kg/s for the 3 km (b) and 5 km (d) DBHEs, respectively. As clearly seen in Figure 6, after 30 years of operation, increasing the flow rate does continue to increase thermal output, but with diminishing returns. For example, in (a), increasing the flow rate from 1 kg/s to 6 kg/s results in a 204 kW increase in thermal output, while increasing it further to 15 kg/s yields only an additional 37 kW. The outlet temperature peaked at 28 °C at 2 kg/s and 40 °C at 3 kg/s for a 3 km and 5km well respectively. After the peaks the outlet temperature decreases more slowly as flow rate increases, similar to the trend observed in the time-based percentage changes. As mentioned above, the thermal output continues to increase beyond these flow rates; but after 6 kg/s with diminishing returns due to the decrease in the temperature gain experienced. These results highlight a trade-off between maximizing thermal output through higher flow rates and maintaining higher outlet temperatures.

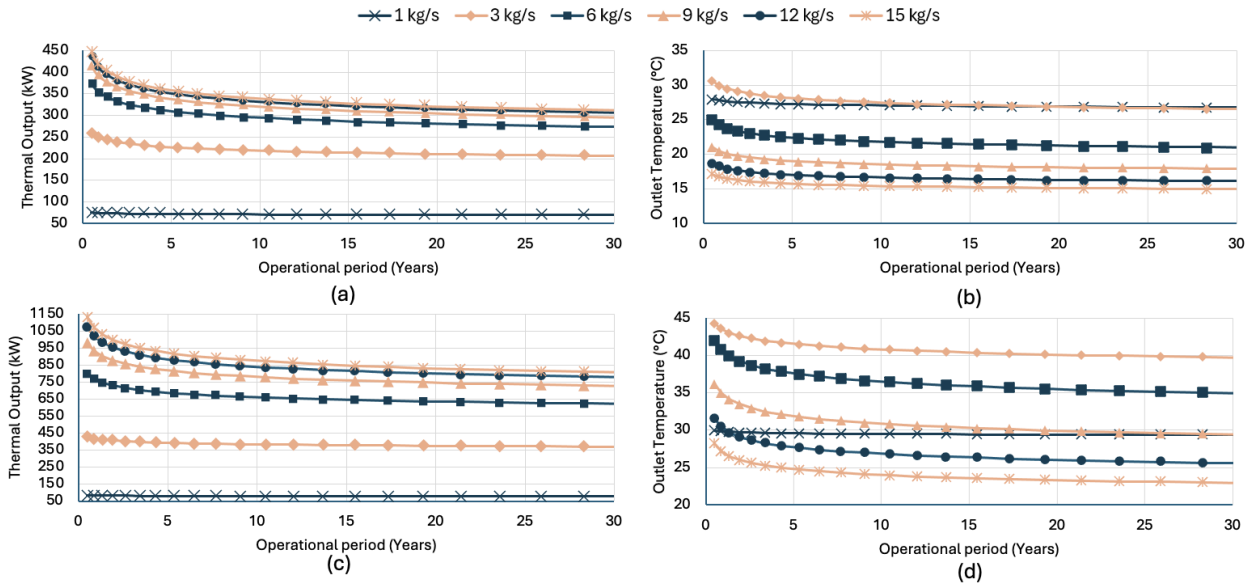

Figure 5: The effect of flow rate on thermal output and outlet temperature for 3 km (a, b) and 5 km (c, d) co-axial DBHEs over a 30-year period, T_{in} = 10 °C, G= 30 K/km, using HDPE internal tubing

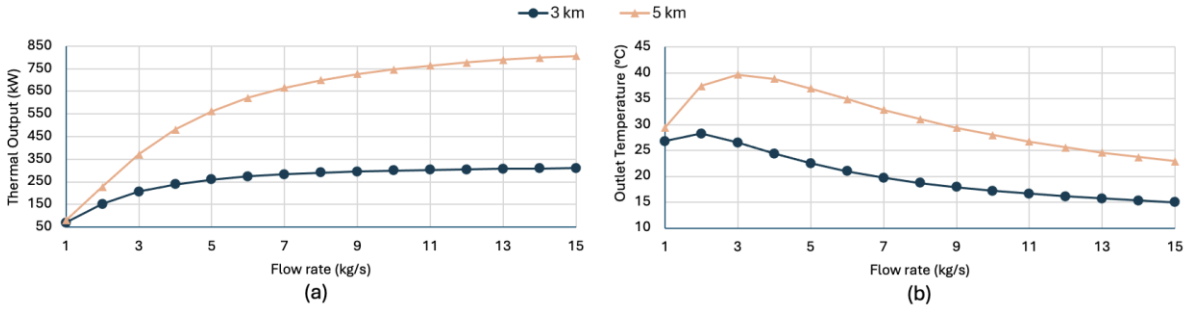

Figure 6: The effect of flow rate on thermal output (a) and outlet temperature for 3 km and 5 km after a 30-year period, T_{in} = 10 °C, G= 30 K/km, using HDPE internal tubing.

3.2. Effect of inlet temperature

Inlet temperatures ranging from 10 °C to 80 °C were investigated. However, for the 3 km well, the upper limit was restricted to 50 °C, as the borehole temperature gain becomes negative when the inlet temperature exceeds the average formation temperature along the borehole depth i.e. with a surface temperature of 12 °C and a geothermal gradient of 30 K/km, the average formation temperature is approximately 57 °C for a 3 km well, compared to 87 °C for a 5 km well. The effect of varying inlet temperature is shown in Figure 7. At both depths, thermal output, depicted in (a) and (c), decreases with increasing inlet temperature. This is primarily due to the reduced temperature difference between the annular fluid and the surrounding formation, which lowers the rate of heat transfer. Additionally, higher inlet temperatures lead to increased heat losses near the surface, where the formation temperature is initially lower than the inlet temperature. This trend is also reflected in the outlet temperature, (b) and (d), where the net temperature gain decreases with higher inlet temperatures. Over the 30-year simulation period, the rate of thermal output decline increased only marginally (<1%) with higher inlet temperatures. The outlet temperature decline rate exhibited the opposite trend i.e. higher inlet temperatures led to lower decline rates. The outlet temperature decreased by approximately 11.6% and 12.5% over 30 years for a 3 km and 5 km DBHE respectively when the inlet temperature was 10 °C, but this reduced to around 1% for the highest inlet temperatures. After 30 years of operation, thermal output increased consistently with each 10 °C step-in inlet temperature by approximately 55 kW for the 3 km well and 80 kW for the 5 km well. Similarly, the outlet temperature increased approximately by 7 - 8 K per 10 °C temperature step for the 3 km and 5 km wells.

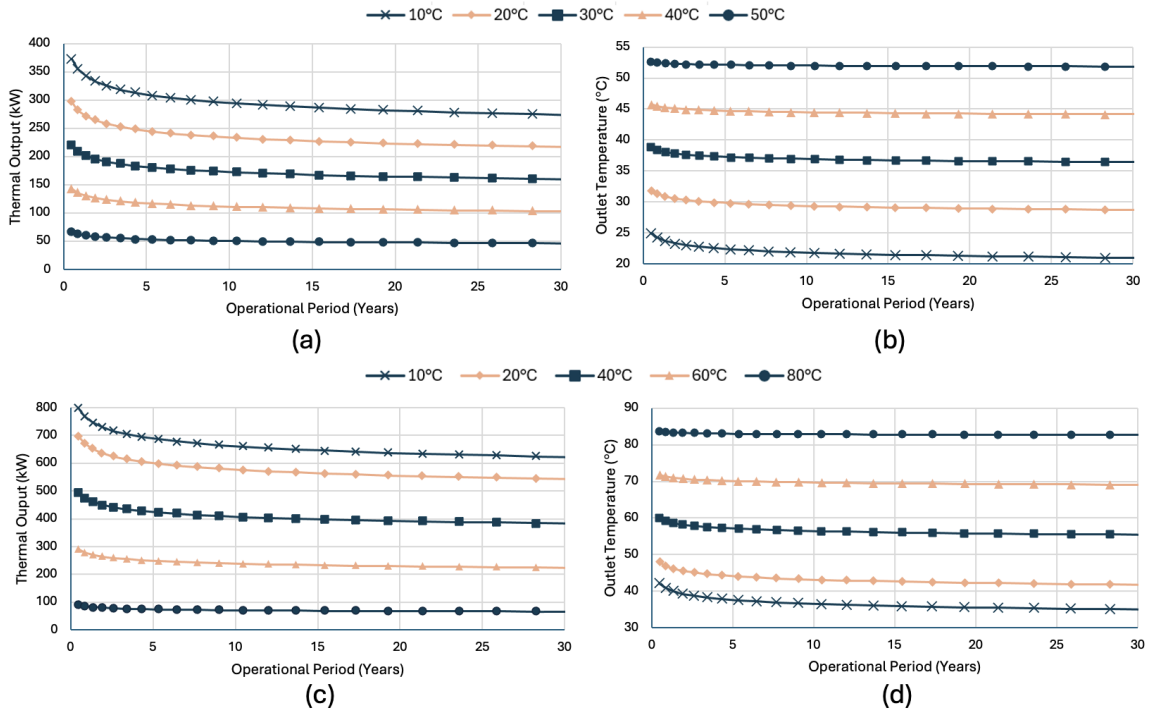

Figure 7: Effect of inlet temperature on thermal output and outlet temperature for 3 km (a, b) and 5 km (c, d) co-axial DBHEs over a 30-year period, m= 6 kg/s and G= 30 K/km, using HDPE internal tubing.

3.3. Effect of thermal gradient

Figure 8 shows the effect of varying the geothermal gradient from 30 K/km to 80 K/km to represent the impact of different global DBHE placements. Increasing the gradient improved system performance significantly, increasing thermal output by a factor of approximately 2.7 for both well depths. Outlet temperature also increased, by a factor of 2.2 and 1.8 for the 3 km (b) and 5 km (d) wells respectively. The rate of thermal output decline over the 30-year period remained unaffected by the change in gradient, staying consistent at 20% for the 3 km well (a) and 17% for the 5 km well (c). The outlet temperature decline was affected but marginally, i.e. increasing slightly with gradient by 4.1% for the 3 km well and 2.4% for the 5 km well.

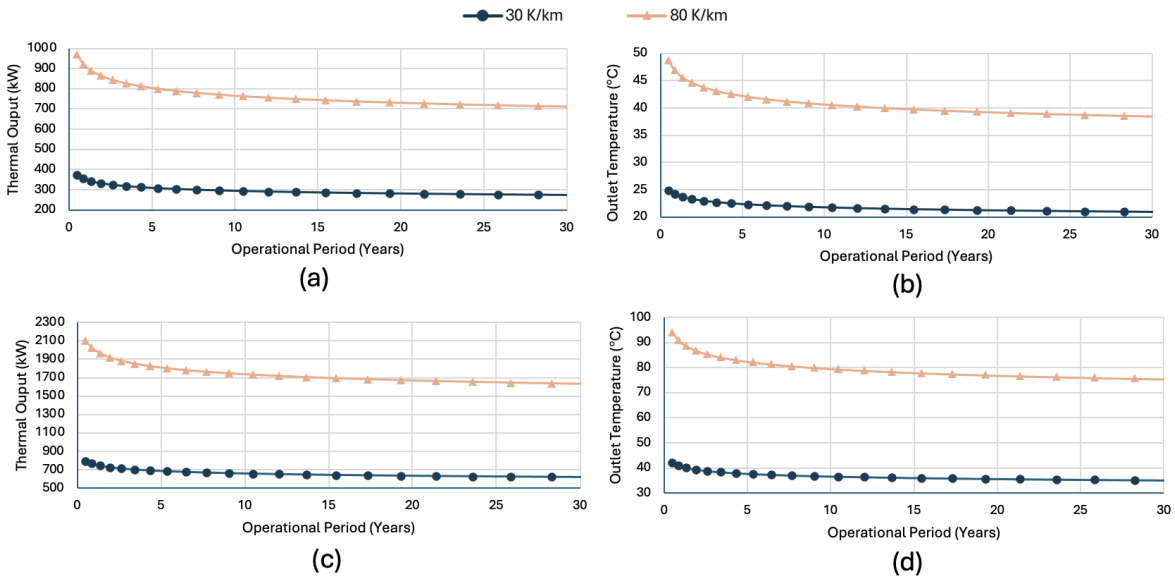

Figure 8: Effect of geothermal gradient on thermal output and outlet temperature for 3 km (a, b) and 5 km

(c, d) co-axial DBHEs over a 30-year period, m= 6 kg/s, T=10 °C, using HDPE internal tubing.

3.4. Effect of internal tubing type

Figure 9 shows the effect of using VIT as opposed to HDPE for the central tubing. VIT was significantly more effective in the 5 km DBHE, where it increased thermal output and outlet temperature by 330 kW and 13 °C, respectively, compared to increases of 56 kW and 2.24 °C for the 3 km well. The use of VIT increased only slightly the rate of decline in performance between 1 and 30 years. For the 3 km DBHE, the thermal output and outlet temperature decline rates increased by only 2%, while for the 5 km DBHE, they increased by 3%.

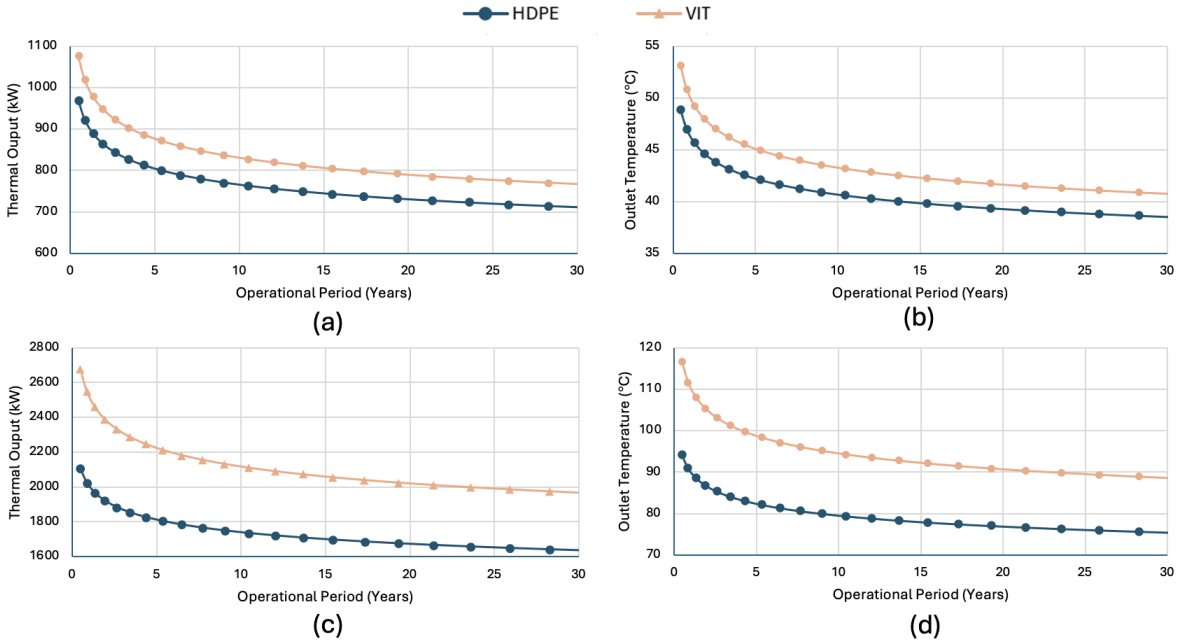

Figure 9: Effect of internal tubing on thermal output and outlet temperature for 3 km (a, b) and 5 km (c, d) co-axial DBHEs over a 30-year period, *at m= 6 kg/s, T=10 °C, and G= 80 K/km*

3.5. Pumping Power

Figure 10 presents the effect of flow rate on pumping power requirements for the 3 km and 5 km DBHEs. At flow rates below 8 kg/s, the 5 km well requires less pumping power than the 3 km. This apparent anomaly is due to the buoyancy effect that is higher for the higher temperature differentials of the 5 km well. However, the pumping power for the 5 km DBHE increases more rapidly with flow rate, eventually exceeding that of the 3 km as expected.

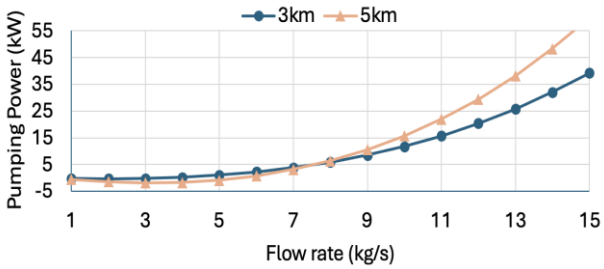

Figure 10: Effect of flow rate on pumping power for 3 km and 5 km co-axial DBHEs, 30-year period, n_p=0.7.

3.6. Heating

The 4th generation heating networks require source temperatures between 50 and 60 °C [23]. In areas of 80 K/km both 3 km and 5 km wells have the potential to provide heating directly. For example, as indicated in Figure 9, and after 30-years of operation, a 5 km geothermal well with a VIT pipe and a geothermal gradient of 80 K/m will be able to deliver 2 MW of thermal output at a temperature of 90 °C, while if we were to reduce the required outlet temperature to 60 °C by increasing the flow rate to 9 kg/s, the same well can deliver 2.1 MW for direct use in heating applications. Similarly for the 3 km DBHE,

although in Figure 9 only 41 °C is obtained, utilising a lower flow rate of 3kg/s can provide 684 kW at 60 °C. DBHEs in a 30 K/km area would require thermal up-grade with a heat pump. Equation 2 below gives the possible heat pump thermal output (Q_h) as a function of the input energy from the geothermal well (Q_s) and the Coefficient of Performance (COP). The COP was obtained from equation 3 as a function of the temperature outlet (T_{out}) of the geothermal plant and the required temperature of the heat network (T_{req}). This equation was derived from data in Kensa, [24]. Taking outputs where the inlet temperature was 10 °C and flow rates of 6 kg/s to maximise the thermal output while keeping pumping power relatively low and a T_{req} = 55 °C, resulted in the heat pump thermal outputs of Table 3.

$$Q_H = \frac{Q_S COP}{COP-1} \quad (2)$$

$$COP = 0.1993T_{out} - 0.0016T_{out}\,T_{req} - 0.051T_{req} + 6.266 \quad (3)$$

Table 3: Heating potential with a heat pump for 3 km and 5 km well depths at 30 K/km after 30 years of operation for an inlet temp of 10℃, flow rate of 6 kg/s and HDPE to provide 55℃ to a heat user.

Depth (km)	3	5
Well Outlet Temp (°C)	21	35
Well Thermal Output (kW)	273	622
COP	5.8	7.3
Heat Pump output (kW)	330	720

Table 4: Optimal well parameters for 3 km and 5 km well depths for different geothermal gradients and their net electrical output after 30 years of operation.

Geothermal gradient (K/km)	30	80	
Well depth (km)	5	3	5
Inlet Temp (°C)	42	25	25
Flow rate (kg/s)	2	2	3
Outlet Temp (°C)	80.1	89.5	144.4
Thermal Output (kW)	316	537.7	1501
Net electrical output (kW)	17.1	33.5	170.3
Efficiency (%)	5.4	6.2	11.3

3.7. Power generation

The efficiency of an Organic Rankine Cycle (ORC) increases with the temperature of the heat source, making higher inlet temperatures more desirable. However, higher thermal outputs also result in a greater amount of energy available for conversion to electricity. While temperature improves efficiency, output thermal energy quantity improves overall power generation potential. Typical ORC systems require a minimum inlet temperature of around 80 °C to operate effectively [25]. The ORC efficiency approximations used in this study are based on the correlation developed by [26], which relates the DBHEs produced fluid temperature (T_{out}) to thermal efficiency. The relationships used are shown in Equation 3 and 4. The minimum and maximum plotted return temperatures to the DBHE of 25 °C and 55 °C were used as the boundaries, similar to [26], for the range in the inlet temperature for the simulations.

$$\dot{W} = \dot{W}_{T_{in}=40\,℃} + \frac{\Delta\dot{W}}{\Delta T}(T_{in} - 40) \quad (3)$$

$$\frac{\Delta\dot{W}}{\Delta T} = 0.098701 - 0.0039645T_{out} \quad (4)$$

Variations for both well depths that supplied an outlet temperature ≥ 80 °C and a VIT installation were included to determine the best net output for an ORC for a low and high geothermal gradient area with both well depths. A 3 km well in a region where the gradient is 30 K/Km was not included due to the DBHE not being able to produce high enough temperatures for electrical generation. Table 4 shows the operating conditions for the largest electrical output, where pumping power was included as a parasitic load in the net output.

4. CONCLUSIONS

This study demonstrated that the performance of a co-axial DBHE depends on both operating parameters and geological placement. Higher initial thermal extraction is achieved through lower inlet temperatures,

high mass flow rates and the use of VIT. However, as a result, the formation surrounding the borehole cools more rapidly, leading to faster local thermal depletion and thus a greater reduction in thermal output over long term operation. It was also seen that there is an optimised flow rate, which increased with well depth, where the temperature outlet peaks, while the thermal output shows diminishing returns. For heating applications, co-axial DBHE's located in areas with higher gradients i.e. 80 K/km, can directly provide the temperatures required by fourth generation heat networks. In areas of lower gradients i.e. 30 K/km, heat pumps would be necessary to upgrade the outlet temperature of the DBHE but still show potential especially with deeper configurations, where increasing the depth from 3 to 5 km showed an increase in thermal output by a factor of 2.1 while still using HDPE tubing. Further optimisation of the heat pump and DBHE as a whole system is required. The ability for electrical generation is limited to areas of higher geothermal gradient i.e. 80 K/km where using VIT is beneficial due to increasing the temperature output which has a positive impact on the efficiency of an ORC. Lower flow rates and inlet temperatures are more conducive for electrical generation in all cases when VIT tubing is used. In conclusion the results highlighted that there is a trade-off between short term performance and long-term stability showing that careful optimisation of inlet temperature, flow rate, and internal pipe design is essential for maximising performance over a 30-year continuous operational lifetime. This optimisation process should include the diameters of the casing and the inner tubing.

5. NOMENCLATURE

D = Diameter (m)
G = geothermal gradient (K/km)
$\dot{m}$ = water mass flow rate (kg/s)
Q_H = Heat pump thermal outlet (kW)
Q_s = Heat pump source thermal input (kW)
T_{in} = Water inlet temperature to the well (^oC)
T_{out} = Water well outlet temperature (^oC)
T_{req} Temperature required by heat network (^oC)
$\dot{W}$ = Specific power output (kW/(kg/s))

Greek Letters

α= Diffusivity (m^2/K)
τ = Time (s)
η_p = pump efficiency
ΔT = Temperature Difference (K)
$\Delta\dot{W}$ = Change in specific power output (kW/(kg/s))

ACKNOWLEDGEMENTS

The financial support of the Engineering and Physical Sciences Research Council under the Doctoral Mobility Programme and and sponsorship from Pennmen ltd for Paige Draper is acknowledged.

REFERENCES

[1] Marquez R, Ovalles C, Lopez-Linares F, Wang W, Robinson P, Reynolds MA. Perspective from the ACS Energy & Fuels Industry Committee toward the Transition to Sustainable Energy Sources. Energy & Fuels. 2025 Jan 23;39(3):1451–9.

[2] International Energy Agency (IEA). World Energy Investment 2025 [Internet]. 2025 [cited 2025 Aug 24]. Available from: https://www.iea.org/reports/world-energy-investment-2025

[3] Giroud A. World Investment Report 2023: Investing in sustainable energy for all. Journal of International Business Policy. 2024 Mar 18;7(1):128–31.

[4] REN21. Renewables 2024 Global Status Report Collection [Internet]. Paris; 2024 [cited 2025 Aug 24]. Available from: https://www.ren21.net/gsr-2024/modules/global_overview/03_investment

[5] Strojny M, Gładysz P, Andresen T, Pająk L, Starczewska M, Sowiżdżał A. Environmental Impact of Enhanced Geothermal Systems with Supercritical Carbon Dioxide: A Comparative Life Cycle Analysis of Polish and Norwegian Cases. Energies (Basel). 2024 Apr 26;17(9):2077.

[6] Ministère de la Transition énergétique. Géothermie : un plan d'action pour accélérer le développement [Internet]. 2023 [cited 2025 Aug 24]. Available from: https://www.ecologie.gouv.fr/presse/geothermie-plan-daction-accelerer

[7] Ministère de l'Économie des F et de la S industrielle et numérique. Géothermie : des mesures concrètes pour accélérer le développement d'une énergie vertueuse [Internet]. 2025 [cited 2025 Aug 24]. Available from: https://presse.economie.gouv.fr/geothermie-des-mesures-concretes-pour-accelerer-le-developpement-dune-energie-vertueuse/

[8] Xiao D, Liu M, Li L, Cai X, Qin S, Gao R, Liu J, Liu X, Tang H, Li G. Model for economic evaluation of closed-loop geothermal systems based on net present value. Appl Therm Eng. 2023 Aug;231:121008.

[9] Chamorro CR, García-Cuesta JL, Mondéjar ME, Pérez-Madrazo A. Enhanced geothermal systems in Europe: An estimation and comparison of the technical and sustainable potentials. Energy. 2014 Feb 1;65:250–63.

[10] Kubačka J, Karayiannis TG. Performance of vacuum-insulated central pipes for deep borehole heat exchangers in geothermal systems. International Journal of Low-Carbon Technologies. 2024;19:2068–85.

[11] Chen H, Shi Y, Liu C, Zhao Z, Yue Y, Li M. Performance comparison of different well configurations for medium-deep coaxial closed-loop geothermal systems. Appl Therm Eng. 2025 Jul;271:126393.

[12] International Energy Agency (IEA). The Future of Geothermal Energy [Internet]. 2023 Nov [cited 2025 Jul 10]. Available from: https://www.iea.org/reports/the-future-of-geothermal-energy

[13] Jello J, Baser T. Utilization of existing hydrocarbon wells for geothermal system development: A review. Appl Energy. 2023 Oct;348:121456.

[14] Liu Z, Yang W, Xu K, Zhang Q, Yan L, Li B, Cai X, Yang M. Research progress of technologies and numerical simulations in exploiting geothermal energy from abandoned wells: A review. Geoenergy Science and Engineering. 2023 May;224:211624.

[15] Zhang J, Zhu X. Productivity evaluation of geothermal energy production system based on abandoned oil and gas wells. In: Utilization of Thermal Potential of Abandoned Wells. Elsevier; 2022. p. 115–34.

[16] Cleantech Group. Geothermal: Drilling Accounts for 75% of Project Cost and 90% of Capital Cost [Internet]. 2024 [cited 2025 Jul 9]. Available from: https://www.cleantech.com/release/geothermal-drilling-accounts-for-75-of-project-cost-and-90-of-capital-cost/

[17] Qiao M, Jing Z, Feng C, Li M, Chen C, Zou X, Zhou Y. Review on heat extraction systems of hot dry rock: Classifications, benefits, limitations, research status and future prospects. Renewable and Sustainable Energy Reviews. 2024 May;196:114364.

[18] Cai X, Liu Z, Xu K, Li B, Yang M. Numerical simulation on converting abandoned wells into double-well open-loop geothermal system. Appl Therm Eng. 2024 Jul;248:123324.

[19] Kubačka J. ON THE THERMAL-HYDRAULIC RESPONSE OF DEEP CLOSED-LOOP WELLBORE SYSTEMS [Internet]. Doctoral dissertation, Brno University of Technology; 2025 [cited 2025 Aug 7]. Available from: https://www.vut.cz/en/students/final-thesis/detail/163087?zp_id=163087

[20] Alimonti C. Technical Performance Comparison between U-Shaped and Deep Borehole Heat Exchangers. Energies (Basel). 2023 Feb 1;16(3).

[21] Kujawa T, Nowak W, Stachel AA. Analysis of the exploitation of existing deep production wells for acquiring geothermal energy. Journal of Engineering Physics and Thermophysics. 2005 Jan;78(1):127–35.

[22] Bu X, Ran Y, Zhang D. Experimental and simulation studies of geothermal single well for building heating. Renew Energy. 2019 Dec 1;143:1902–9.

[23] Wiltshire R, Jentsch A, Gullev L. DISTRICT HEATING GENERATIONS – CLARIFICATION OF THE TERM [Internet]. DBDH. 2024 [cited 2025 Aug 9]. Available from: https://dbdh.org/district-heating-generations-clarification-of-the-term/

[24] Kensa. Actual Outputs TIS [Internet]. [cited 2025 May 21]. Available from: https://cdn.sanity.io/files/lnwa68k7/production/b113debf325127e0399bca04b141e4c5349d8ba3.pdf

[25] Exergy. Organic Rankine Cycle System [Internet]. 2022 [cited 2025 Aug 8]. Available from: https://www.exergy-orc.com/technology/orc/

[26] Idaho National Laboratory. The future of geothermal energy : Impact of Enhanced Geothermal Systems (EGS) on the United States in the 21st century [Internet]. Massachusetts Institute of Technology; 2006 [cited 2025 Apr 24]. Chapter 7. Available from: https://energy.mit.edu/wp-content/uploads/2006/11/MITEI-The-Future-of-Geothermal-Energy.pdf

A DIGITAL TWIN OF THE NISYROS VOLCANO: ENABLING EDUCATION AND AWARENESS THROUGH IMMERSIVE TECHNOLOGIES AND REAL-TIME MONITORING

Prof. Nancy Alonistioti[1], C.J. Koroneos[2], Konstantinos Sorras[1]

[1]Dept. of Informatics and Telecommunications, National and Kapodistrian University of Athens
[2] Municipality of Nisyros
e-mail: nancy@di.uoa.gr

ABSTRACT

Volcanoes are emblematic natural phenomena with profound implications for ecosystems, societies, and sustainable development. Leveraging recent advances in immersive technologies and real-time data integration, this work presents the design and implementation of a digital twin of the Nisyros volcano in Greece, conceived as both a scientific and educational tool. The proposed digital twin combines high-fidelity 3D reconstruction of the volcanic landscape, created through drone-based photogrammetry, with live environmental monitoring from an array of in-situ sensors measuring temperature, gas emissions, etc. The resulting virtual model is realized in the Unity engine, providing an interactive and visually engaging representation of the volcano that mirrors its current state and dynamic behavior. Beyond its scientific value for hazard awareness and monitoring, the platform is designed to support educational activities at primary, secondary, and tertiary levels. Pupils and students can explore the volcano's geology, understand its processes, and observe real-time changes through an accessible, gamified interface, fostering environmental literacy and awareness of natural risks. By coupling cutting-edge digital twin technologies with sustainability-oriented education, the initiative demonstrates how digital innovation can enhance resilience and promote informed engagement with natural heritage sites.

Keywords: Digital twin, Nisyros volcano, photogrammetry, Unity, environmental sensors, education, sustainability, real-time monitoring

1. INTRODUCTION

In addition to providing a scientifically accurate representation of the Nisyros volcano, the platform is designed to enhance environmental awareness and foster proactive attitudes among pupils and students. By transforming real-time sensor data into an intuitive, gamified experience, the digital twin engages learners in exploring the dynamic processes of the volcano. Students can monitor temperature fluctuations and gas emissions as they happen, and are challenged to interpret the data, predict trends, and propose mitigation strategies within the virtual environment.

This interactive approach bridges theoretical knowledge with tangible phenomena, making the invisible processes of the Earth more relatable and impactful. Gamification elements—such as progress badges for correctly identifying risk scenarios, collaborative missions to “prepare” the virtual island for an environmental challenge, and leaderboards promoting friendly competition— encourage sustained engagement and deepen understanding.

By actively participating in monitoring and decision-making within the simulated environment, students develop critical thinking, data literacy, and a sense of responsibility toward natural risk management and sustainability. Furthermore, the immersive 3D experience strengthens their connection to local natural heritage, cultivating a culture of respect and preparedness. This pedagogical approach aligns with the principles of education for sustainable development, empowering young generations to become informed, active stakeholders in addressing environmental challenges.

2. METHODOLOGY

2.1. Data Collection and 3D Reconstruction

The foundation of the digital twin is a high-fidelity 3D reconstruction of the Nisyros volcanic landscape. Drone-based photogrammetry is employed to capture high-resolution images of the caldera, fumaroles, and surrounding terrain. These datasets are processed into textured 3D meshes, ensuring scientific accuracy and visual realism.

Figure 1: Digital Twin with time lapse projection capability (what-if scenarios)

2.2. Sensor Network and Real-Time Monitoring

An array of in-situ sensors is deployed across the volcano to capture real-time environmental data. Measurements include ground temperature, gas composition (SO_2, CO_2), and atmospheric conditions. Data is transmitted wirelessly to a central server, where it is processed and integrated into the digital twin.

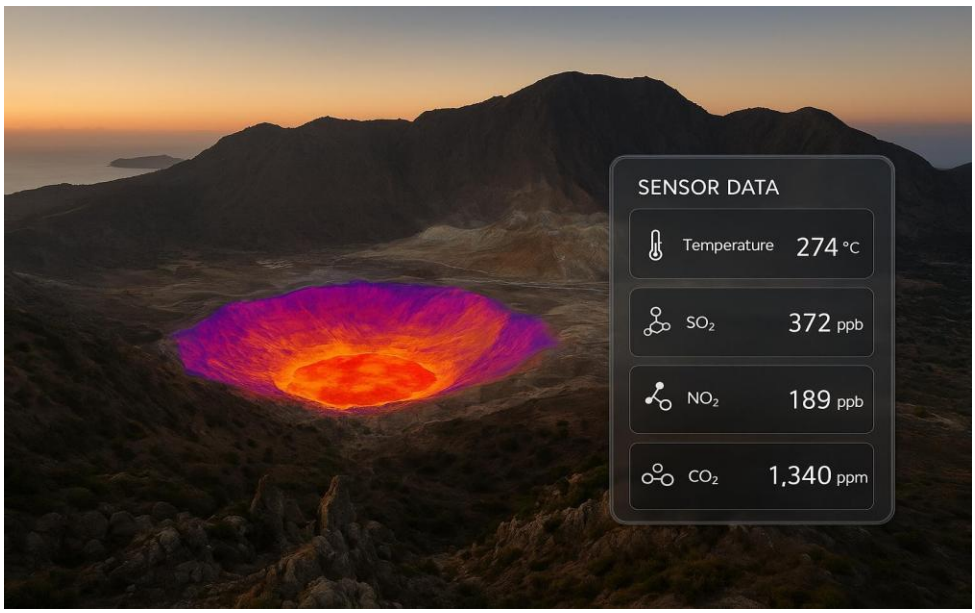

Figure 2: Digital Twin with integrated real time sensing visualization

2.3. Platform Development

The digital twin is implemented using the Unity game engine, enabling an interactive and immersive experience. Real-time data feeds update the virtual environment dynamically, allowing users to visualize current volcanic activity.

2.4. Educational Integration and Gamification

The platform incorporates gamified learning modules designed for multiple education levels. Primary school pupils interact through simplified exploration tasks, while advanced users engage with data interpretation challenges and scenario-based risk management exercises.

The educational framework addressed by the design of the platform can be summarized in the following aspects.

2.4.1. Experiential Learning Capabilities

1. Immersive Exploration of Volcanic Processes
    1.1. Students can virtually “walk” through the crater, explore fumaroles, and witness thermal and gas emissions in real time.
    1.2. Complex processes like magma movement, gas release, and geothermal gradients are visualized interactively, making abstract concepts tangible.
2. Data Literacy & Scientific Reasoning
    2.1. Real-time sensor feeds (temperature, SO_2, NO_2, CO_2, seismic data) allow students to analyze authentic datasets.
    2.2. They can practice interpreting time-series data, identifying anomalies, and correlating environmental changes with volcanic risk.
3. Scenario-Based Learning & Risk Simulation

3.1. Students can engage in simulations of eruption scenarios and test mitigation strategies (e.g., evacuation planning, gas emission alerts).

3.2. This promotes systems thinking, decision-making under uncertainty, and applied sustainability education.

4. Gamification for Engagement

4.1. Missions (e.g., “detect the SO_2 spike before it exceeds safe limits”) and collaborative challenges encourage teamwork and problem-solving.

4.2. Gamified rewards (badges, progress tracking, leaderboards) sustain motivation and participation.

5. Cross-Disciplinary Applications

5.1. Combines geology, physics, environmental science, and sustainability policy, allowing for project-based interdisciplinary learning.

5.2. Higher education students can extend this into research, data modeling, or policy evaluation tasks.

3. RESULTS

The integration of real-time sensor data with immersive visualization produces a virtual model that accurately reflects the volcano’s condition. Pilot studies with secondary school students will be demonstrated for increased engagement and retention of volcanic science concepts compared to traditional textbook-based teaching.

Gamified features—such as progress tracking, collaborative challenges, and feedback mechanisms— will be addressed in terms of effectiveness in motivating students to explore more deeply. Teachers will report KPIs related to improved student understanding of volcanic processes, risk awareness, and sustainability concepts.

The Key Performance Indicators (KPIs) for Student Engagement have been identified by an interdisciplinary approach and are the initial outcomes for the introduction of digital twins as educational tools for environmental learning.

To assess the effectiveness of the digital twin in learning, the following KPIs can be measured:

1. Engagement Metrics

1.1. Session Duration: Average time spent in the simulation.

1.2. Interaction Rate: Number of active interactions (sensor checks, data queries, virtual movement).

1.3. Completion of Missions/Tasks: Percentage of gamified learning modules completed.

2. Learning Outcomes

2.1. Knowledge Gain: Pre- and post-assessment quizzes on volcanology and sustainability concepts.

2.2. Data Analysis Accuracy: Correct interpretation of sensor data (e.g., identifying trends, predicting risks).

2.3. Critical Thinking: Quality of written or oral responses in decision-making exercises.

3. Motivation & Satisfaction
    3.1. Self-Reported Engagement: Surveys using Likert-scale responses on enjoyment and perceived learning.
    3.2. Return Rate: Frequency of students revisiting the platform voluntarily.
4. Skill Development
    4.1. Digital Literacy: Ability to navigate immersive environments and data dashboards.
    4.2. Research Skills: Engagement in independent exploration, hypothesis formulation, and analysis.

In short, the volcano digital twin fosters experiential, inquiry-driven, and gamified learning while enabling measurable KPIs that educators can use to track progress and refine teaching strategies.

4. CONCLUSIONS

This study highlights the potential of digital twin technologies to transform environmental education and risk awareness. The Nisyros volcano digital twin will not only advance scientific monitoring but also democratizes access to complex data through an intuitive, interactive interface. By fostering experiential learning and gamification, the platform enables the promotion of environmental literacy, critical thinking, and resilience.

Future work will focus on scaling conducting trials for educational purposes and extend the platform to include historical data, visualization of past conditions and structural characteristics and developing multilingual educational content to broaden accessibility.

ACKNOWLEDGEMENTS

The authors would like to thank the Municipality of Nisyros for their support.

REFERENCES

[1] Alonistioti, N., Koroneos, C.J., “Smart Nisyros: A digital twin-empowered platform for the detection, management and mitigation of hazardous events,” SUST 2024.

[2] Unity Technologies. “Unity Real-Time Development Platform.” 2024.

[3] Zoe Wakeford, Magda Chmielewska, Malcolm Hole, John Howell, Dougal A. Jerram, “Combining thermal imaging with photogrammetry of an active volcano using UAV: an example from Stromboli, Italy”, December 2019, The Photogrammetric Record 34(168):445- 466, DOI:10.1111/phor.12301.

[4] UNESCO, “Education for Sustainable Development Goals,” 2021.

NISYROS GEOPARK: A LIVING LABORATORY OF VOLCANIC GEOHERITAGE AND SUSTAINABILITY IN THE SOUTH AEGEAN

Paraskevi Nomikou[1], Elisavet Nikoli[2], Evangelos Tasioulas[2], Christofis Koroneos[3], Kalliopi Sakkali[2], Georgios Koukourakis[2], Panagiotis Nastos[1], Varvara Antoniou[1], Dimitrios Emmanouloudis[3], George Pehlivanides[4], Aris Batis[5]

[1]National and Kapodistrian University of Athens
[2] Municipal Public Benefit Enterprise of Nisyros (DIKEN)
[3] International Hellenic University
[4](hands-on studio), Research & Art Direction, Branding, UX/UI Design, Project Management
[5] Econtent Systems P.C, Software, Website and Mobile application development
e-mail: evinom@geol.uoa,gr

ABSTRACT

Nisyros Geopark, located in the Southeastern Aegean and currently a candidate for UNESCO Global Geopark status, offers a compelling model of integrated sustainability in an insular context. Spanning 481 km² and centered around the active Nisyros volcano and nearby islets, it is a vibrant living laboratory of volcanic geoheritage, environmental resilience, and cultural continuity. As part of the South Aegean Volcanic Arc—one of the most active and scientifically significant volcanic systems globally—the geopark exemplifies the interdependence of natural processes and human adaptation.

The geopark comprises 24 distinct geosites, showcasing a dynamic terrestrial and submarine volcanic landscape formed over five eruptive cycles across 160,000 years. Visitors and researchers alike can explore collapse calderas, hydrothermal craters, lava domes, and coastal hot springs, as well as underwater volcanic features such as craters and the prehistoric Avyssos caldera. These geological phenomena support international research while simultaneously shaping local identity and livelihoods.

Crucially, the geopark is not only a geological asset but also a cultural and ecological one. It hosts centuries-old fortresses, Byzantine monasteries, and ancient thermal baths that reflect a deep historical connection to the landscape. Rich in biodiversity, the area is protected under two Natura 2000 designations and three national wildlife refuges, supporting endemic flora and fauna and reinforcing ecological stewardship.

Socially and economically, the Geopark supports resilient local communities through sustainable tourism, education, and cultural preservation. Ongoing initiatives include mobile applications (Nisyros Geopark App, Nisyros Volcano App), educational programs, workshops, and media outreach, all designed to enhance public engagement and environmental awareness.

As a case study, Nisyros Geopark illustrates the synergistic potential of sustainability's four pillars. It embodies an integrative approach to climate resilience, ecological protection, cultural heritage conservation, and community empowerment, making it a model for sustainable development in small island contexts facing the challenges of the Anthropocene.

Laboratory of Soft Energy Applications & Environmental Protection (SEALAB)

Tel. 0030-2105381237 and 0030-2105381020

Optimisation of Production Systems Laboratory (OPS)

Tel. 0030-2105381430

Address: University of West Attica, Olive Grove Campus, P. Ralli and Thivon 250, Egaleo 12244 Websites: www.sealab.gr, www.ops.mech.uniwa.gr, www.mbaenergy.gr, www.oilgasmsc.gr **Nisyros Municipality**

www.nisyros.gr, tel : 00302242360501